

Lawrence Berkeley National Laboratory

LBL Publications

Title

Ultra-low emittance beam generation using two-color ionization injection in a CO₂ laser-driven plasma accelerator:

Permalink

<https://escholarship.org/uc/item/1h74s8tg>

Authors

Schroeder, Carl
Benedetti, Carlo
Bulanov, Stepan
et al.

Publication Date

2017-12-05

Ultra-low emittance beam generation using two-color ionization injection in a CO₂ laser-driven plasma accelerator

C. B. Schroeder^a, C. Benedetti^a, S. S. Bulanov^a, M. Chen^b, E. Esarey^a, C. G. R. Geddes^a,
J.-L. Vay^a, L.-L. Yu^b, W. P. Leemans^a

^aLawrence Berkeley National Laboratory, Berkeley, California 94720, USA;

^bShanghai Jiao Tong University, Shanghai 200240, China

May 21, 2015

ABSTRACT

Ultra-low emittance (tens of nm) beams can be generated in a plasma accelerator using ionization injection of electrons into a wakefield. An all-optical method of beam generation uses two laser pulses of different colors. A long-wavelength drive laser pulse (with a large ponderomotive force and small peak electric field) is used to excite a large wakefield without fully ionizing a gas, and a short-wavelength injection laser pulse (with a small ponderomotive force and large peak electric field), co-propagating and delayed with respect to the pump laser, to ionize a fraction of the remaining bound electrons at a trapped wake phase, generating an electron beam that is accelerated in the wake. The trapping condition, the ionized electron distribution, and the trapped bunch dynamics are discussed. Expressions for the beam transverse emittance, parallel and orthogonal to the ionization laser polarization, are presented. An example is shown using a 10- μm CO₂ laser to drive the wake and a frequency-doubled Ti:Al₂O₃ laser for ionization injection.

Keywords: Laser plasma accelerator, ionization injection, CO₂ laser

1. INTRODUCTION

Plasma-based accelerators¹ can produce extremely large accelerating gradients, enabling compact sources of high-energy beams. Rapid experimental progress has occurred in the field of laser-driven plasma accelerators, and electron beams accelerated to multi-GeV energies have been demonstrated^{2,3} using an intense laser driving a plasma wave in cm-scale plasmas. Generation of these electron beams relied on self-injection from the background plasma in highly-nonlinear plasma waves.⁴ In the regime where background plasma electrons are self-trapped, experiments show that beams with sub-micron normalized transverse emittance can be produced.^{5,6}

To reduce the electron beam emittance further it has been proposed to use a laser to ionize electrons at a trapped phase in a plasma wake that is independently excited by a particle beam⁷ or an intense laser.⁸ The laser-based method⁸ relies on two laser pulses of different colors: a long wavelength pulse, with large ponderomotive force and small peak electric field, excites a plasma wake without fully ionizing a high-Z gas; a short-wavelength injection pulse, with small ponderomotive force and large peak electric field, co-propagating and delayed with respect to the wake drive laser, ionizes a fraction of the remaining bound electrons at a trapping phase of the wake, generating an electron beam. Figure 1 illustrates the basic principle of the two-color ionization injection method. This two-color, two-pulse ionization injection concept was first proposed in Ref. 9. An additional numerical study was performed in Ref. 10 subsequent to Refs. 8,9.

In this paper we discuss the trapping condition, the distribution of ionized electrons, and the dynamics of the trapped electron beam. We present expressions for the transverse emittance, parallel and orthogonal to the laser polarization, of the trapped electron beam, valid for beam or laser wakefield drivers.¹¹ For the all-optical, two-color ionization injection method, it is natural to consider a 10- μm CO₂ laser as the long-wavelength drive pulse, generating the plasma wake, followed by a Ti:Al₂O₃ laser (frequency-doubled, with 0.4 μm wavelength) for ionization injection. Progress in CO₂ laser technology has opened the possibility of sub-ps pulse durations, that would enable efficient (i.e., resonant, with duration of order the plasma period) plasma wakefield excitation at plasma densities $\sim 10^{16}$ cm⁻³, and such laser systems are expected to become available in the next several years.¹² We present an example of two-color ionization injection using a short-pulse, CO₂ drive laser pulse and a frequency-doubled, Ti:Al₂O₃ injection laser pulse.

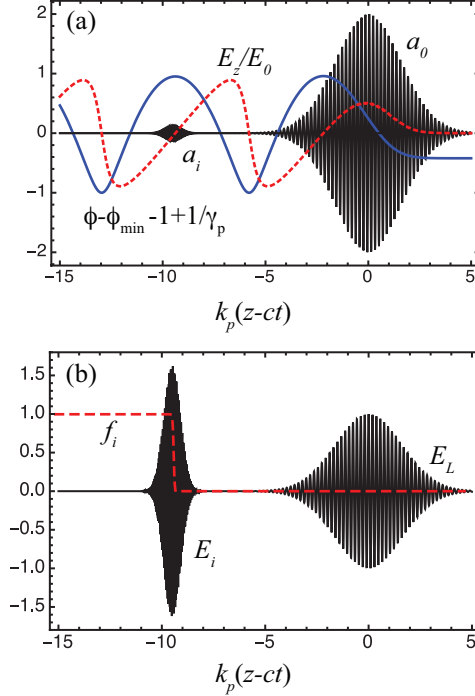


Figure 1. (a) Drive laser vector potential a_0 , ionization laser vector potential a_i , excited plasma wakefield E_z/E_0 (red dashed curve), and trapping condition $0 < \phi - \phi_{\min} - 1 + 1/\gamma_p$ (blue curve). (b) Drive (E_L) and ionization (E_i) laser electric fields (normalized to the peak of E_L) and the fraction of the high-Z gas state ionized f_i (red dashed curve).

2. TRAPPING PHYSICS

2.1 Trapping condition

The two-color ionization injection concept relies on a large plasma wave (or wakefield) excited by a long-wavelength drive laser pulse, with wavelength $\lambda_0 = 2\pi/k_0$ and normalized vector potential amplitude $a_0 = eA_0/m_e c^2$, where e and m_e are the electron charge and mass, respectively, and c is the speed of light. For efficient wakefield generation the drive pulse should be approximately resonant with the plasma, with $k_p L_0 \sim 1$, where L_0 is the drive laser length and $\omega_p = k_p c = (4\pi e^2 n_e / m_e)^{1/2}$ is the plasma frequency, with n_e the electron number density. Co-propagating and delayed with respect to the drive pulse is an ionization laser pulse, with wavelength $\lambda_i = 2\pi/k_i < \lambda_0$ and normalized vector potential amplitude $a_i = eA_i/m_e c^2$. The ionization pulse electric field $E_i = (2\pi m_e c^2 / e) a_i / \lambda_i$ is sufficiently large, $a_i / \lambda_i \gtrsim a_0 / \lambda_0$, to ionize remaining bound electrons in the gas, that may be trapped in the wakefield.

Trapping requires that the electrons are ionized at the proper wake phase and that the wake amplitude is sufficiently large. Behind the drive laser pulse, and assuming $a_i^2(\psi_i) \ll 1$, this condition may be expressed as¹³

$$1 - \gamma_p^{-1} \leq \phi(\psi_i) - \phi_{\min}, \quad (1)$$

where $\psi_i = k_p \xi = k_p(z - ct)$ is the phase position in the plasma wakefield of the ionized electron (initially at rest), with γ_p is the Lorentz factor of the plasma wave phase velocity, and ϕ is the potential of the wakefield (normalized to $m_e c^2 / e$), with ϕ_{\min} in the minimum amplitude of the potential. Here we have assumed the wakefield near the axis is approximately described by the 1D nonlinear wake potential,¹ whose extrema satisfy,

$$\phi_{\min/\max} = (E_z/E_0)^2/2 \pm \beta_p \left\{ [1 + (E_z/E_0)^2/2]^2 - 1 \right\}^{1/2}, \quad (2)$$

where E_z/E_0 is the peak of the accelerating wakefield normalized to $E_0 = m_e c^2 k_p / e$. The optimal ionization phase ψ_i for trapping is at the peak of the wake potential, $\phi(\psi_i) = \phi_{\max}$ and $E_z(\psi_i) = 0$. At this phase location,

the trapping condition is $1 - \gamma_p^{-1} \leq \phi_{\max} - \phi_{\min}$. In the limit $\gamma_p \gg 1$, the minimum wakefield amplitude required for trapping is

$$E_z/E_0 \geq (\sqrt{5} - 2)^{1/2} \simeq 0.49. \quad (3)$$

The longitudinal wakefield amplitude excited by a resonant, circularly-polarized, Gaussian laser pulse is $E_z/E_0 \simeq (\pi/2e)^{1/2} a_0^2 (1 + a_0^2)^{-1/2}$, such that the required laser amplitude for trapping is $a_0 > 0.94$.

Figure 1 illustrates an example of the concept of two-color ionization injection. Figure 1(a) shows the drive laser vector potential a_0 (pulse centered at the origin), the field of the excited plasma wake E_z/E_0 (red dashed curve), the ionization laser vector potential [pulse centered at $k_p(z - ct) \simeq -9.5$] $a_i \ll a_0$, and the trapping condition Eq. (1), where $0 \leq \phi - \phi_{\min} - 1 + 1/\gamma_p$ indicates an electron ionized at rest will be trapped (blue curve). Figure 1(b) shows the electric field of the drive and ionization lasers (normalized to the peak drive laser field), and the fraction of the ionized gas state f_i (red dashed curve). The normalized parameters shown in Fig. 1 correspond to the case of a 10- μm wavelength (CO₂) drive laser, with $a_0 = 2$ (linear polarization) and 0.47 ps duration (FWHM laser intensity), propagating in a uniform gas, producing a plasma with electron density $n_e = 10^{16} \text{ cm}^{-3}$, and resonantly exciting a wakefield. The ionization pulse, with $a_i = 0.13$ (linear polarization), $\lambda_i = 0.4 \mu\text{m}$ (frequency-doubled Ti:Al₂O₃ laser), and 120 fs duration (FWHM intensity), ionizes Kr⁸⁺ to Kr⁹⁺ (ionization potential $U_i = 230 \text{ eV}$) at a trapped wake phase.

2.2 Trapped charge

Tunneling ionization will determine the distribution of electrons ionized, and, hence the trapped charge and emittance. The transverse phase space distribution of the ionized electrons was derived in Ref. 11. The rms radius of the transverse distribution of ionized electrons is¹¹

$$\sigma_x = \sigma_y \simeq (w_i/\sqrt{2})\Delta, \quad (4)$$

where w_i is the ionization laser spot size [i.e., $\mathbf{a}_i = a_i \exp(-r^2/w_i^2)\hat{\mathbf{x}}$] and

$$\Delta = \left(\frac{3\pi r_e a_i}{\alpha^4 \lambda_i} \right)^{1/2} \left(\frac{U_H}{U_I} \right)^{3/4}, \quad (5)$$

where $r_e = e^2/m_e c^2$ is the classical electron radius, α is the fine structure constant, and U_i is the potential of the state of the gas used for ionization injection, normalized to $U_H \simeq 13.6 \text{ eV}$. The parameter Δ^2 is the normalized laser field amplitude $E_i \propto a_i/\lambda_i$, and $\Delta^2 \ll 1$ is satisfied at the ionization threshold. (Here we assume the Keldysh parameter $\gamma_K = [2U_i/(m_e c^2 a_i^2)]^{1/2}$ satisfies $\gamma_K < 1$, such that tunneling ionization is the dominant ionization mechanism.)

For an ionization laser pulse located at the proper phase ψ_i of a plasma wave of sufficient amplitude E_z/E_0 , given by Eq. (1), electrons ionized at rest will be on trapped orbits, and the amount of trapped charge will be determined by the number of ionized electrons: $N_t = 2\pi\sigma_x\sigma_y\ell_i f_i n_g$, where f_i is the ionization fraction, n_g is the number of ions with electrons in the proper charge state, and ℓ_i is the interaction length. For interaction with a single species gas, $n_g = n_e/Z$, where n_e is the electron density and Z is the number of electrons ionized by the drive laser (or pre-ionized). If the length of the high- Z gas region is longer than the ionization laser Rayleigh range, then the total charge will be limited by the diffraction of the ionizing laser, $\ell_i \sim Z_{Ri} = \pi w_i^2/\lambda_i$, and, hence, we expect the charge to scale as $Q = eN_t \simeq e(\pi w_i^2 \Delta^2)\ell_i f_i n_g \propto w_i^4$ with the interaction length limited by diffraction. As shown below, the emittance scales as $\epsilon \propto w_i^2$, and, hence, there is a trade-off between increasing the trapped charge ($N_t \propto w_i^4$, limited by diffraction) and reducing the emittance.

3. EMITTANCE

The achievable beam emittance using ionization injection into a wakefield, driven by a charged particle beam or an intense laser, is determined by the initial phase space distribution of the trapped electrons and the plasma focusing forces.¹¹ The rms of the momentum distribution of the ionized electrons, in the plane of laser polarization, is approximately¹¹

$$\sigma_{p_x} \simeq a_i \Delta, \quad (6)$$

where Δ is given by Eq. (5). For a small ionization injection laser amplitude $a_i^2 \ll 1$, the momentum gain from the ponderomotive force of the ionizing laser may be neglected. Using Eqs. (4) and (6), the initial thermal emittance of the beam generated by ionization injection is¹¹

$$\epsilon_t = \left(\frac{3\pi r_e}{\sqrt{2}\alpha^4} \right) \left(\frac{U_H}{U_i} \right)^{3/2} \frac{w_i a_i^2}{\lambda_i}. \quad (7)$$

Equation (7) is independent of the driver of the plasma accelerator (e.g., laser or particle beam) and is determined from the ionization physics, i.e., the distribution of electrons produced via tunneling ionization. Unless injected matched, the emittance of the trapped beam will grow due to phase mixing in the plasma wakefield.

3.1 Trapped particle dynamics

An electron trapped in the plasma wakefield, i.e., ionized at the proper phase to satisfy the trapping condition Eq. (1), will begin to accelerate and rotate in transverse phase space. For an electron with initial transverse position x_0 and normalized momentum u_0 , the transverse position and momentum will evolve as

$$x \simeq \gamma^{-1/4} [x_0 \cos(k_\beta z) + (u_0/k_{\beta 0}) \sin(k_\beta z)] = \gamma^{-1/4} r_{\beta 0} \cos(k_\beta z + \varphi), \quad (8)$$

$$u_x = p_x/m_e c \simeq \gamma^{1/4} [u_0 \cos(k_\beta z) - x_0 k_{\beta 0} \sin(k_\beta z)] = -\gamma^{1/4} k_{\beta 0} r_{\beta 0} \sin(k_\beta z + \varphi), \quad (9)$$

where $r_{\beta 0} = [x_0^2 + (u_0/k_{\beta 0})^2]^{1/2}$ is the initial betatron amplitude, the energy $\gamma(z)$ is increasing as the electron is accelerated in the wakefield, $k_\beta \propto \gamma^{-1/2}$ is the betatron wavenumber in the wakefield, and $k_{\beta 0} = k_\beta(z=0)$ is the initial betatron wavenumber. For laser drivers with parameters satisfying $a_0(1+a_0^2)^{-1/4} \gtrsim k_p w_0/2$ (assuming circular polarization), or particle beam drivers, the driver will produce a co-moving ion cavity with $k_\beta \simeq k_p/\sqrt{2}\gamma$.

Averaging the betatron amplitude over the initial beam distribution yields¹¹

$$\langle r_{\beta 0}^2 \rangle = \sigma_x^2 + \sigma_{p_x}^2/k_{\beta 0}^2 = \left[1 + \frac{2a_i^2}{(k_{\beta 0} w_i)^2} \right] w_i^2 \Delta^2/2 \quad (10)$$

in the plane of ionization laser polarization, and $\langle r_{\beta 0}^2 \rangle = w_i^2 \Delta^2/2$ orthogonal to the plane of laser polarization.

If the ionization injection region is short (due to a finite high-Z gas region or short ionization injection pulse Rayleigh range), followed by a post acceleration region that is sufficiently long to allow betatron phase mixing, then the normalized emittance will saturate to

$$\epsilon = [\langle x^2 \rangle \langle u_x^2 \rangle - \langle x u_x \rangle^2]^{1/2} = k_{\beta 0} \langle r_{\beta 0}^2 \rangle / 2. \quad (11)$$

The initial beam phase-space distribution Eq. (10) will determine the final saturated emittance Eq. (11). Matched injection in the plane of laser polarization, where the thermal emittance Eq. (7) equals the saturated emittance Eq. (11), occurs for laser-plasma parameters such that $k_{\beta 0} w_i = \sqrt{2} a_i$. If continuous ionization injection occurs over the length of the plasma accelerator, the saturated emittance will asymptote to $\epsilon = k_{\beta 0} \langle r_{\beta 0}^2 \rangle / \sqrt{3}$.

4. TWO-COLOR IONIZATION INJECTION EXAMPLE

In this Section we present an example of beam generation using two-color ionization injection with a short-pulse CO₂ laser driving the wakefield and a frequency-doubled Ti:Al₂O₃ ionizing laser. Modeling was done using the INF&RNO¹⁴ and WARP¹⁵ PIC codes of BLAST (Berkeley Lab Accelerator Simulation Toolkit).¹⁶ Figure 2 shows the evolution of the transverse normalized emittance of the trapped electron beam versus propagation distance z . In Fig. 2, a 10 μm -wavelength, 10 J, CO₂ laser with $a = 2$ (linear polarization), 0.47 ps duration (FWHM laser intensity), and 155 μm spot size ($Z_R = 7.5$ mm) propagates in Krypton gas, ionizing the gas up to Kr⁸⁺, producing a plasma with electron density 10^{16} cm^{-3} (gas density of $n_g = 1.25 \times 10^{15} \text{ cm}^{-3}$) and driving a wake. A frequency-doubled (0.4 μm wavelength) Ti:Al₂O₃ laser with $a_i = 0.14$ (linear polarization), 120 fs duration (FWHM laser intensity), $w_i = 20 \mu\text{m}$ spot size ($Z_{Ri} = 3$ mm), delayed with respect to the CO₂ laser, ionizes Kr⁸⁺ to Kr⁹⁺ ($U_i = 230$ eV) and generates a trapped electron beam. The solid black and red solid curves are the

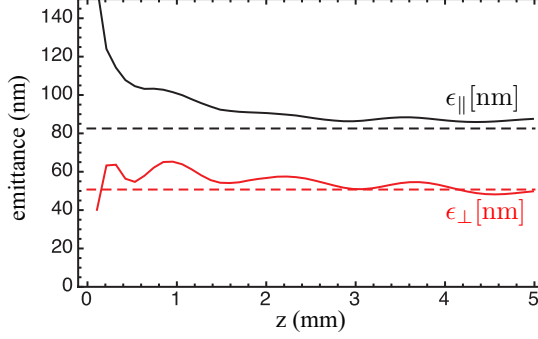


Figure 2. Example of two-color ionization injection using CO₂ drive laser: A (10 μm wavelength) 10 J, CO₂ laser with $a = 2$ (linear polarization), 0.47 ps duration (FWHM laser intensity), and 155 μm spot size ($Z_R = 7.5$ mm) propagates in Krypton gas, ionizing the gas up to Kr⁸⁺, producing a plasma with electron density 10^{16} cm⁻³ and driving a wake. A frequency-doubled (0.4 μm wavelength) Ti:Al₂O₃ laser with $a_i = 0.14$ (linear polarization), 120 fs duration (FWHM laser intensity), $w_i = 20$ μm spot size ($Z_{Ri} = 3$ mm), delayed with respect to the CO₂ laser, ionizes Kr⁸⁺ to Kr⁹⁺ ($U_i = 230$ eV) and generates a trapped electron beam. Evolution of the transverse normalized emittance of the trapped electron beam versus propagation distance z (mm) is plotted: (black curve) emittance in the laser polarization plane from PIC simulation, (dashed black line) ϵ_{\parallel} theoretical saturated emittance in the laser polarization plane Eq. (12), (red curve) emittance orthogonal to the laser polarization plane from PIC simulation, and (dashed red line) ϵ_{\perp} theoretical saturated emittance orthogonal to the laser polarization plane Eq. (13).

normalized transverse emittance of the trapped electron beam, parallel and orthogonal to the laser polarization plane, respectively, calculated using the INF&RNO module of BLAST.

For a small ionization injection laser amplitude $a_i^2 \ll 1$, propagating in a uniform gas jet, the final normalized transverse emittances¹¹ are, using Eqs. (11), (10), and (5),

$$\epsilon_{\parallel} = k_{\beta 0} w_i^2 \left[1 + \frac{2a_i^2}{(k_{\beta 0} w_i)^2} \right] \frac{a_i}{\lambda_i} \left(\frac{3\pi r_e}{4\alpha^4} \right) \left(\frac{U_H}{U_i} \right)^{3/2}, \quad (12)$$

$$\epsilon_{\perp} = k_{\beta 0} w_i^2 \frac{a_i}{\lambda_i} \left(\frac{3\pi r_e}{4\alpha^4} \right) \left(\frac{U_H}{U_i} \right)^{3/2}, \quad (13)$$

where ϵ_{\parallel} (ϵ_{\perp}) is the transverse normalized emittance parallel (orthogonal) to the plane of ionization laser polarization. Shown in Fig. 2 are the theoretical predictions: (dashed black line) ϵ_{\parallel} emittance in the laser polarization plane Eq. (12) and (dashed red line) ϵ_{\perp} emittance orthogonal to the laser polarization plane Eq. (13). For these drive laser-plasma parameters, $k_{\beta 0}/(k_p/\sqrt{2}) \simeq 0.9$. Good agreement is achieved between the PIC simulation and the theoretical estimates Eqs. (12) and (13). Phase mixing is not complete after 5 mm, and the emittance orthogonal to the plane of laser polarization is still varying. The charge contained in the beam modeled with the PIC code is 27 pC. This approximately agrees with the order-of-magnitude estimate of the trapped charge over a Rayleigh length, assuming $f_i \approx 1$,

$$Q = eN_t \sim en_g Z_{Ri} \pi w_i^2 \Delta^2, \quad (14)$$

which, for the parameters of Fig. 2, yields $Q \simeq 34$ pC.

In general, a trade-off exists between the reducing the emittance ($\epsilon \propto w_i^2$) and increasing the trapped charge ($Q \propto w_i^4$, with interaction length limited by diffraction). Figure 3 shows the theoretical estimates for the beam emittance [parallel, Eq. (12) (dashed black curve), and orthogonal, Eq. (13) (dashed red curve), to the ionization laser polarization] and the charge, Eq. (14) (dashed blue curve) versus ionization laser spot size (all other parameters are the same as Fig. 2). The points in Fig. 3 are PIC simulation results (calculated using the INF&RNO module of BLAST) for the emittance in the laser polarization plane ϵ_{\parallel} [nm] (black) and orthogonal to the laser polarization plane ϵ_{\perp} [nm] (red), and the charge Q [pC] (blue).

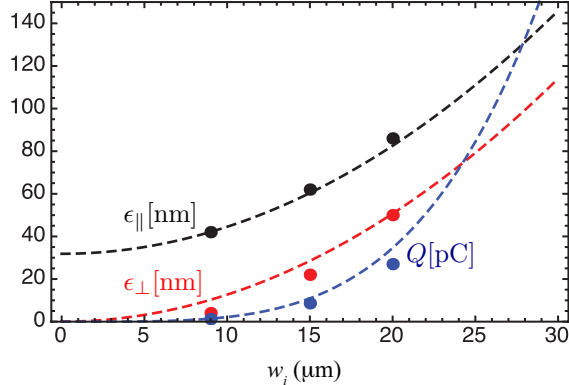


Figure 3. Emittance [parallel, Eq. (12) (dashed black curve), and orthogonal, Eq. (13) (dashed red curve), to the ionization laser polarization] and the charge Eq. (14) (dashed blue curve) versus ionization laser spot size (all other parameters are the same as Fig. 2). Points are PIC simulation results for the emittance parallel ϵ_{\parallel} [nm] (black) and orthogonal ϵ_{\perp} [nm] (red) to the laser polarization, and the charge Q [pC] (blue).

5. SUMMARY AND CONCLUSIONS

Ultra-low emittance electron beams, on the order of tens of nm, can be generated in a plasma accelerator using ionization injection in a wakefield.^{7,8,11} In this paper we have reviewed the trapping physics, distribution of ionized electrons, and the trapped beam dynamics. Expressions for the achievable beam emittance using ionization injection into a plasma wakefield were presented.¹¹ Note that these results are independent of the wakefield driver (laser⁸ or particle beam⁷). An experimentally-relevant example was presented of ultra-low emittance beam generation by two-color ionization injection using a short-pulse, CO₂ laser driving the wakefield and a frequency-doubled, Ti:Al₂O₃ laser ionizing a Krypton gas. In this example the interaction region was limited by the Rayleigh range of the ionizing laser. In general, a trade-off exists between the reducing the saturated emittance ($\epsilon \propto w_i^2$) and increasing the trapped charge ($N_t \propto w_i^4$, with interaction length limited by diffraction). Self-consistent numerical modeling of the beam injection for this example was performed and compared to analytic estimates, showing good agreement. It should be noted that this example is not fully optimized, and, depending on the laser-plasma parameters, other gases may be considered (e.g., Ne) for improved performance.

ACKNOWLEDGMENTS

This work was supported by the Director, Office of Science, Office of High Energy Physics, of the U.S. Department of Energy under Contract Nos. DE-AC02-05CH11231. This research used computational resources of the National Energy Research Scientific Computing Center, which is supported by the Office of Science of the U.S. Department of Energy under Contract No. DE-AC02-05CH11231. This work was supported in part by the National Basic Research Program of China (Grant No. 2013CBA01504) and the National Natural Science Foundation of China (Grant No. 11405107).

REFERENCES

1. E. Esarey, C. B. Schroeder, and W. P. Leemans, “Physics of laser-driven plasma-based electron accelerators,” *Rev. Mod. Phys.* **81**, pp. 1229–1285, July–September 2009.
2. X. Wang, R. Zgadaj, N. Fazel, Z. Li, S. A. Yi, X. Zhang, W. Henderson, Y.-Y. Chang, R. Korzekwa, H.-E. Tsai, C.-H. Pai, H. Quevedo, G. Dyer, E. Gaul, M. Martinez, A. C. Bernstein, T. Borger, M. Spinks, M. Donovan, V. Khudik, G. Shvets, T. Ditmire, and M. C. Downer, “Quasi-monoenergetic laser-plasma acceleration of electrons to 2 GeV,” *Nature Communications* **4**, p. 1988, June 2013.
3. W. P. Leemans, A. J. Gonsalves, H.-S. Mao, K. Nakamura, C. Benedetti, C. B. Schroeder, C. Tóth, J. Daniels, D. E. Mittelberger, S. S. Bulanov, J.-L. Vay, C. G. R. Geddes, and E. Esarey, “Multi-GeV

- electron beams from capillary-discharge-guided subpetawatt laser pulses in the self-trapping regime,” *Phys. Rev. Lett.* **113**, p. 245002, December 2014.
4. C. Benedetti, C. B. Schroeder, E. Esarey, F. Rossi, and W. P. Leemans, “Numerical investigation of electron self-injection in the nonlinear bubble regime,” *Phys. Plasmas* **20**, p. 103108, October 2013.
 5. G. R. Plateau, C. G. R. Geddes, D. B. Thorn, M. Chen, C. Benedetti, E. Esarey, A. J. Gonsalves, N. H. Matlis, K. Nakamura, C. B. Schroeder, S. Shiraishi, T. Sokollik, J. van Tilborg, Cs. Tóth, S. Trotsenko, T. S. Kim, M. Battaglia, T. Stöhlker, and W. P. Leemans, “Ultra-low-emittance electron bunches from a laser-plasma accelerator measured using single-shot x-ray spectroscopy,” *Phys. Rev. Lett.* **109**, p. 064802, August 2012.
 6. R. Weingartner, S. Raith, A. Popp, S. Chou, J. Wenz, K. Khrennikov, M. Heigoldt, A. R. Maier, N. Kajumba, M. Fuchs, B. Zeitler, F. Krausz, S. Karsch, and F. Grüner, “Ultralow emittance electron beams from a laser-wakefield accelerator,” *Phys. Rev. ST Accel. Beams* **15**, p. 111302, November 2012.
 7. B. Hidding, G. Pretzler, J. B. Rosenzweig, T. Königstein, D. Schiller, and D. L. Bruhwiler, “Ultracold electron bunch generation via plasma photocathode emission and acceleration in a beam-driven plasma blowout,” *Phys. Rev. Lett.* **108**, p. 035001, January 2012.
 8. L.-L. Yu, E. Esarey, C. B. Schroeder, J.-L. Vay, C. Benedetti, C. G. R. Geddes, M. Chen, and W. P. Leemans, “Two-color laser-ionization injection,” *Phys. Rev. Lett.* **112**, p. 125001, March 2014.
 9. L.-L. Yu, E. Esarey, J.-L. Vay, C. B. Schroeder, C. Benedetti, C. G. R. Geddes, S. G. Rykovanov, S. S. Bulanov, M. Chen, and W. P. Leemans, “Low transverse emittance electron bunches from two-color laser-ionization injection,” in *Proc. SPIE*, **8779**, p. 877908, SPIE Digital Library, May 2013.
 10. X. L. Xu, Y. P. Wu, C. J. Zhang, F. Li, Y. Wan, J. F. Hua, C.-H. Pai, W. Lu, P. Yu, C. Joshi, and W. B. Mori, “Low emittance electron beam generation from a laser wakefield accelerator using two laser pulses with different wavelengths,” *Phys. Rev. ST Accel. Beams* **17**, p. 061301, June 2014.
 11. C. B. Schroeder, J.-L. Vay, E. Esarey, S. S. Bulanov, C. Benedetti, L.-L. Yu, M. Chen, C. G. R. Geddes, and W. P. Leemans, “Thermal emittance from ionization-induced trapping in plasma accelerators,” *Phys. Rev. ST Accel. Beams* **17**, p. 101301, October 2014.
 12. I. V. Pogorelsky and I. Ben-Zvi, “Brookhaven National Laboratory’s Accelerator Test Facility: Research Highlights and Plans,” *Plasma Phys. Control. Fusion* **56**, p. 084017, July 2014.
 13. M. Chen, E. Esarey, C. B. Schroeder, C. G. R. Geddes, and W. P. Leemans, “Theory of ionization-induced trapping in laser-plasma accelerators,” *Phys. Plasmas* **19**, p. 033101, March 2012.
 14. C. Benedetti, C. B. Schroeder, E. Esarey, C. G. R. Geddes, and W. P. Leemans, “Efficient modeling of laser-plasma accelerators with INF&RNO,” in *Proc. of 2010 Advanced Accelerator Concepts Workshop*, G. Nusinovich and S. Gold, eds., **1299**, pp. 250–255, AIP, (NY), 2010.
 15. J.-L. Vay, D. P. Grote, R. H. Cohen, and A. Friedman, “Novel methods in the particle-in-cell accelerator code-framework warp,” *Comput. Sci. Discovery* **5**, p. 014019, 2012.
 16. “Berkeley Lab Accelerator Simulation Toolkit.” <http://blast.lbl.gov>.

DISCLAIMER

This document was prepared as an account of work sponsored by the United States Government. While this document is believed to contain correct information, neither the United States Government nor any agency thereof, nor the Regents of the University of California, nor any of their employees, makes any warranty, express or implied, or assumes any legal responsibility for the accuracy, completeness, or usefulness of any information, apparatus, product, or process disclosed, or represents that its use would not infringe privately owned rights. Reference herein to any specific commercial product, process, or service by its trade name, trademark, manufacturer, or otherwise, does not necessarily constitute or imply its endorsement, recommendation, or favoring by the United States Government or any agency thereof, or the Regents of the University of California. The views and opinions of authors expressed herein do not necessarily state or reflect those of the United States Government or any agency thereof or the Regents of the University of California.